Theoretical derivation of slip boundary conditions for single-species gas and binary gas mixture

Jun Zhang ⬤,[*] Peng Luan ⬤, Junchao Deng, and Peng Tian
School of Aeronautic Science and Engineering, Beihang University, Beijing 100191, China

Tengfei Liang
School of Astronautics, Northwestern Polytechnical University, Xi'an 710072, China

A theoretical derivation of slip boundary conditions for single-species gas and binary gas mixture based on two typical gas-surface scattering kernels is presented. If the Maxwell model is assumed, then the derived slip boundary conditions are consistent with the previous conclusions. Considering the limitation of the Maxwell model in describing the complexity of gas-surface scattering behavior, we further perform theoretical analyses based on the Cercignani-Lampis-Lord (CLL) model, where separate accommodation coefficients in the tangential and normal directions are defined. Our results demonstrate that for both single-species gas and binary gas mixture, the velocity slip predicted by the CLL model is only dependent on the tangential accommodation coefficient, while the temperature jump determined by the CLL model is related to the accommodation coefficients in both tangential and normal directions. To account for the collision effect in the Knudsen layer, we propose to add correction terms to the theoretical models, and the corrected slip coefficients agree well with the previous numerical results obtained by solving Boltzmann equation for single-species gas. Moreover, the slip boundary conditions for binary gas mixture based on the CLL model are determined theoretically for the first time. Since at most situations the tangential and normal accommodation coefficients are not equal, the temperature jump boundary condition based on the CLL model is expected to give more accurate predictions about temperature distribution and heat flux at the boundaries, particularly for hypersonic gas flows with strong nonequilibrium effect.

I. INTRODUCTION

Aerodynamic design of aircraft requires accurate and refined prediction of its surrounding flow fields and surface properties such as drag force, lift force, and heat flux. This requirement is challenging for advanced hypersonic vehicles, such as reusable spacecraft, single stage to orbit vehicles, and hypersonic gliders, as they encounter significantly various flow regimes in different altitudes due to the change of atmospheric density [1,2]. Generally, aerodynamic design of such hypersonic vehicles needs comprehensive analyses by incorporating flight experiments, wind tunnel testing, and numerical simulation. While the first two methods are expensive and technically challenging, numerical simulation can be performed with relatively low cost even under extreme conditions.

Computational fluid dynamics (CFD) has played a vital role in the prediction of aerodynamic performance and hence boost the development of aerodynamic design during the past half century. The validity and reliability of CFD calculations rely upon not only the numerical algorithms for solving governing equations but also the underlying physical models including constitutive relations and boundary conditions [3–6]. If the vehicles fly at low altitudes, then the gas flow

is in the continuum regime represented by a small Knudsen number (Kn), i.e., Kn < 0.001. Generally, Kn is defined as the ratio of the molecular mean free path, which is inversely proportional to the density, to the concerned length in the system. It is believed that in the continuum regime, the flow fields can be obtained using conventional CFD methods, which numerically solve the Navier-Stokes-Fourier (NSF) equations in conjunction with linear constitutive relations and no-slip boundary conditions.

On the contrary, when the hypersonic vehicles fly to higher altitudes, the number of intermolecular collisions in the flow fields becomes much smaller due to lower atmospheric density. In this case, nonequilibrium gas effect needs to be considered [7]. It is recognized that for Kn > 0.1, which is referred to rarefied flow regime, the description by the traditional CFD methods with linear constitutive relations is less accurate and in some cases even wrong. Instead, the numerical methods by solving the Boltzmann equation [8,9] or alternatively, using the stochastic particle description like the direct simulation Monte Carlo (DSMC) method [10,11], can provide accurate predictions under this condition. However, both methods are computationally expensive for the slip regime with mediate Knudsen numbers, e.g., 0.001 < Kn < 0.1. In this case, CFD methods using appropriate slip boundary conditions have been demonstrated to be a promising strategy to correctly predict nonequilibrium behavior to some extent with a much lower computational cost

---
[*]jun.zhang@buaa.edu.cn

compared to molecular-based calculations [3,12–14]. There-fore, it is preferred particularly for engineering applications in the slip regime.

Maxwell [15] was the first to propose a slip boundary condition for a flat surface. According to his theory, the slip velocity is determined by a slip coefficient multiplied by the velocity gradient normal to the surface. Gökçen and MacCormack [16] found that the surface properties predicted by such a simple boundary condition for large Knudsen numbers might significantly deviate from that determined by the theory for free-molecular flow. Hence, they extended the Maxwell model and proposed a general model which could also give correct predictions for large Knudsen numbers. Although the first-order model is not perfect, it is still the most widely used model so far. In contrast, a variety of second-order slip models with two free parameters [17–22] have also been developed, but the values of the parameters for a specific problem are still under discussion.

Alternatively, Myong [23] proposed a slip model on the basis of the theory of Langmuir isotherm adsorption. While it has been successfully applied to low-speed micro gas flows, the prediction for hypersonic rarefied gas flows is not so good. Le *et al.* [24,25] improved this kind of boundary condition and extend its application to hypersonic flows. In addition, another kind of slip model was developed by scaling the relationship between stress and strain rate, in order to correctly capture the structure of the Knudsen layer. It is generally represented in terms of correction function, such as wall function [26], power-law scaling [27], and double-power series [28,29]. Note that these scaling functions are determined by the curve-fitting on the basis of kinetic theory or DSMC calculations. These two kinds of boundary conditions are out of the scope of the present work.

According to the kinetic theory, the form of the slip boundary conditions and the associated slip coefficients are dependent on the underlying physics of gas-surface interactions. It is known that the two ideal models for describing gas-surface interactions are specular and diffuse reflections. Maxwell [15] introduced one parameter called as accommodation coefficient (AC), to characterize the degree to which the molecule adapts to the wall. Its value is in the range of 0 to 1, with the lower and upper limits corresponding to completely specular and diffuse reflection, respectively. For a specific gas-surface interaction model with a determined AC, the slip boundary conditions can be determined theoretically using the so-called half-flux method based on the kinetic theory. This method was proposed by Patterson and then developed by Shidlowsky (for reviews, see Ref. [9]). Afterwards, Scott [30] and Gupta *et al.* [31] employed the similar method and extended the application to multicomponent reacting flow. Their researches inspired a lot of follow-up studies by others [32–34].

It should be noted that all the aforementioned boundary conditions, derived by the half-flux method, contain only one AC except the recent work of Struchtrup [35]. However, both experiments [36,37] and molecular dynamics simulations [38,39] have demonstrated that, the Maxwell model with only one AC is inadequate to represent all the behaviors of the gas-surface interactions. An advanced and sophisticated gas-surface interaction model, including two separate ACs for
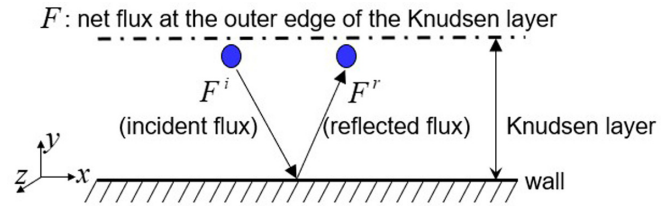

FIG. 1. Schematic of the gas behavior within the Knudsen layer, where the intermolecular collisions are neglected. The net flux is evaluated with the distribution function at the top of the Knudsen layer. The blue solid circle denotes one molecule impinging on the surface with a incident flux and rebounded back with a reflected flux depending on the gas-surface interaction model.

tangential and normal directions, is the so-called Cercignani-Lampis-Lord (CLL) model [40–42]. It has been proved that the CLL model is capable of capturing the scattering behavior of the reflected molecules very well, particularly, the lobular distribution as reported by experimental and molecular dynamics simulation results [36,43,44].

Since the CLL model is more reliable to describe the gas-surface interactions, a natural question that arises is: what are the corresponding slip boundary conditions based on the CLL model? To answer this question, we extend the previous theoretical derivations based on the Maxwell model to the CLL model. Our derived results for the single-species gas are consistent with the conclusion given by Struchtrup [35], albeit he did not provide the details of derivation. To account for the effect of molecular collisions, we propose to add correction factors to the original theoretical models, and the predictions by the corrected models are consistent with previous numerical results. Moreover, we extend the theoretical derivation to binary gas mixture. To the best of our knowledge, the slip boundary conditions for binary gas mixture based on the CLL model has not been reported in the literature yet.

II. SLIP BOUNDARY CONDITIONS FOR SINGLE-SPECIES GAS

For any gas flows around a solid surface, there is a so-called Knudsen layer close to the surface, as shown in Fig. 1. The thickness of the Knudsen layer is about several molecular mean free paths, so the intermolecular collisions could be neglected within the layer but the effect gas-surface interactions becomes dominant. It is well recognized that in the slip regime, if the values of velocity slip and temperature jump are assigned properly, then the conventional CFD method is capable of predicting gas flows outside the Knudsen layer, albeit the prediction within the Knudsen layer may be incorrect.

Strictly speaking, the accurate slip coefficients in any slip boundary conditions need to be determined on the basis of resolving the Knudsen layer, either solving the Boltzmann equation or using DSMC method with proper gas models [45–47]. However, this would be a massive work as numerical solving of the Boltzmann equation is computationally very expensive and a large number of cases need to be run for a complete parametric study. For a comprehensive review of the slip coefficients, we refer the readers to Ref. [48]. Alternatively, a theoretical method called as half-flux method

is a promising way to derive the slip boundary conditions and the associated slip coefficients. It assumes that within the Knudsen layer, the intermolecular collisions are negligible and the behavior of the gas is governed by the gas-surface interaction and free transport of gas molecules. As demonstrated by Struchtrup [35] and Wu and Struchtrup [34], the slip coefficients determined by this method agree well with those determined by solving Boltzmann equation. Therefore, the half-flux method is employed in this work to derive the slip boundary conditions due to its simplicity and acceptable accuracy.

As shown in Fig. 1, the half-flux method assumes that the momentum and energy fluxes are constant in the Knudsen layer. It means that the net flux (F) at the top of the Knudsen layer is equal to the total flux on the wall, which is composed of the incident flux (F^i) and the reflected flux (F^r), that is,

$$F = F^i + F^r. \tag{1}$$

For a property $\phi(\mathbf{C}')$ such as molecular momentum and energy, which can be convected due to molecular movements, the net flux of it at the top of the Knudsen layer in the normal direction is

$$F = \int_{-\infty}^{\infty}\int_{-\infty}^{\infty}\int_{-\infty}^{\infty} V'\phi(\mathbf{C}')f^s(\mathbf{C}') \, d\mathbf{C}', \tag{2}$$

where the vector $\mathbf{C}'$ denotes molecular thermal velocity or peculiar velocity, which is equal to the molecular velocity minus the macroscopic velocity. The three components of $\mathbf{C}'$ in the Cartesian coordinates (x, y, z), as shown in Fig. 1, are denoted as U', V', W', respectively, and $f^s(\mathbf{C}')$ is the distribution function.

Similarly, the incident flux on the wall can be obtained by integrating over the corresponding half-space in molecular velocity, i.e.,

$$F^i = \int_{-\infty}^{\infty}\int_{-\infty}^{0}\int_{-\infty}^{\infty} V'\phi(\mathbf{C}')f^s(\mathbf{C}')d\mathbf{C}', \tag{3}$$

where the incident distribution function is assumed to the same as that at the top of the Knudsen layer. On the contrary, the reflected flux from the wall is more complicated, as the reflected distribution function needs to be determined by the gas-surface scattering kernel. In the following, we will provide theoretical derivations of the slip boundary conditions for the specific gas-surface scattering kernels including the Maxwell model and the CLL model.

A. Slip boundary conditions for single-species gas based on the Maxwell model

The Maxwell model assumes that the reflected flux is caused by a sum of α portion of diffuse reflection and $(1-\alpha)$ portion of specular reflection, and α is the accommodation coefficient (AC). Hence, Eq. (1) can be written as

$$F = F^i + (1-\alpha)F^{sp} + \alpha F^w. \tag{4}$$

Specifically, the specularly and diffusely reflected flux can be obtained as

$$F^{sp} = \int_{-\infty}^{\infty}\int_{0}^{\infty}\int_{-\infty}^{\infty} V'\phi(\mathbf{C}')f^s(U', -V', W') \, d\mathbf{C}', \tag{5}$$

$$F^w = \int_{-\infty}^{\infty}\int_{0}^{\infty}\int_{-\infty}^{\infty} V'\phi(\mathbf{C}')f^w(\mathbf{C}') \, d\mathbf{C}'. \tag{6}$$

Note that f^w is the distribution function at the wall and hence can be evaluated by the Maxwellian form (f^M) due to diffuse reflection, that is,

$$f^w = f^M = n\frac{\beta^3}{\pi^{3/2}} \exp\left(-\beta^2 C'^2\right), \tag{7}$$

where n is the number density and β is the reciprocal of the most probable thermal speed, i.e., $\beta = \sqrt{\frac{m}{2kT}}$. Here m denotes molecular mass, k is the Boltzmann constant, and wall temperature T_w is used for the calculation of β in Eq. (7) to determine f^w.

Now we can apply Eq. (4) to derive the slip velocity. To this end, the convected property is chosen as the molecular momentum in the x direction, i.e., $\phi = m(u_s + U')$. Note that u_s is the macroscopic gas velocity at the top of the Knudsen layer and is virtually the slip velocity associated with NSF equations. To estimate a variety of fluxes, the key step is to determine the distribution function and then perform integrations over the corresponding velocity space. Considering that the NSF equations is essentially the first-order approximation of the Boltzmann equation in terms of Chapman-Enskog expansion, so it is consistent to employ the first-order distribution function for the derivation of the slip boundary conditions. For simplicity, we suppose that the macroscopic velocity varies only in the y direction, i.e., $u_0 = u_0(y)$, and neglect any temperature variation, and hence the Chapman-Enskog distribution function with the first-order form can be written as

$$f^s = f^M\left[1 - \frac{4\mu\beta^4}{\rho}U'V'\frac{\partial u_0}{\partial y}\right], \tag{8}$$

where μ is the dynamic viscosity coefficient and ρ is the mass density.

Substituting $\phi = m(u_s + U')$ and Eq. (8) for f^s into Eq. (3), we can obtain the incident flux as

$$F^i = \int_{-\infty}^{\infty}\int_{-\infty}^{0}\int_{-\infty}^{\infty} V'm(u_s + U')f^M\left[1 - \frac{4\mu\beta^4}{\rho}U'V'\frac{\partial u_0}{\partial y}\right]d\mathbf{C}'$$
$$= -\frac{n\overline{C'}}{4}mu_s - \frac{1}{2}\mu\frac{\partial u_0}{\partial y}, \tag{9}$$

where $\overline{C'}$ denotes the average value of the molecular thermal speed, i.e., $\overline{C'} = \sqrt{\frac{8kT}{\pi m}}$. For brevity, we just provide the result and the details of integration are provided in the Appendix. According to the definitions for the net flux [Eq. (2)], the specularly reflected flux [Eq. (5)], and the diffusely reflected flux [Eq. (6)], similar integrations provide the results as follows:

$$F = -\mu\frac{\partial u_0}{\partial y}, \tag{10}$$

$$F^{sp} = -F^i, \tag{11}$$

$$F^w = 0. \tag{12}$$

Substituting Eqs. (9)–(12) into Eq. (4), we have

$$-\mu\frac{\partial u_0}{\partial y} = \alpha\left(-\frac{n\overline{C'}}{4}mu_s - \frac{1}{2}\mu\frac{\partial u_0}{\partial y}\right). \tag{13}$$

Reformulating the above equation, we can obtain the theoretical formula of the slip velocity, that is,

$$u_s = \frac{2-\alpha}{\alpha} \frac{2\mu}{nm\overline{C'}} \frac{\partial u_0}{\partial y} = \frac{2-\alpha}{\alpha} \frac{\mu\beta\sqrt{\pi}}{\rho} \frac{\partial u_0}{\partial y}. \quad (14)$$

Next we derive temperature jump condition based on the Maxwell model. In this case, we focus on the transport of molecular translational energy, i.e., $\phi = \frac{1}{2}mC'^2$. For simplicity, we suppose that the temperature varies only in the y direction, i.e., $T = T(y)$, and neglect any velocity variations, then Chapman-Enskog distribution function with the first-order form can be written as

$$f^s = f^M \left[1 - \frac{4\kappa\beta^2}{5nk} \left(\beta^2 C'^2 - \frac{5}{2} \right) V' \frac{1}{T} \frac{\partial T}{\partial y} \right], \quad (15)$$

where κ is the coefficient of thermal conductivity. Substituting Eq. (15) into Eq. (3) and using the results of basic integrals provided in Appendix, we can obtain the incident flux of energy as

$$\begin{aligned}
E^i &= \int_{-\infty}^{\infty} \int_{-\infty}^{0} \int_{-\infty}^{\infty} V' \frac{1}{2} mC'^2 f^M \\
&\quad \times \left[1 - \frac{4\kappa\beta^2}{5nk} \left(\beta^2 C'^2 - \frac{5}{2} \right) V' \frac{1}{T} \frac{\partial T}{\partial y} \right] d\mathbf{C}' \\
&= -\frac{n\overline{C'}}{4} 2kT - \frac{1}{2}\kappa \frac{\partial T}{\partial y}.
\end{aligned} \quad (16)$$

Similarly, the net energy flux, the specularly reflected energy flux, and the diffusely reflected energy flux are determined as

$$E = -\kappa \frac{\partial T}{\partial y}, \quad (17)$$

$$E^{sp} = -E^i, \quad (18)$$

$$E^w = \frac{n\overline{C'}}{4} 2kT_w. \quad (19)$$

Substituting Eqs. (16)–(19) into Eq. (4), we have the temperature jump condition as

$$T - T_w = \frac{2-\alpha}{\alpha} \frac{\kappa}{kn\overline{C'}} \frac{\partial T}{\partial y}. \quad (20)$$

B. Slip boundary conditions for single-species gas based on the CLL model

It can been seen from Eqs. (14) and (20) that the slip coefficients in the boundary conditions based on the Maxwell model are dependent on the accommodation coefficient (AC). Once the specific AC is obtained using experimental technique or molecular dynamics simulation, the slip models are completely determined. However, it has been demonstrated that the Maxwell model contains just one AC and hence is not accurate enough to describe scattering behavior of the reflected molecules at some situations. The CLL model which employs two ACs to independently determine the reflected velocities in the tangential and normal directions, has demonstrated its advantage in describing molecular scattering behavior at the kinetic level.

According to kinetic theory, the scattering kernel $P_{\mathrm{CLL}}(\mathbf{c}' \rightarrow \mathbf{c})$, which represents the probability of a gas

molecule with a incident velocity vector $\mathbf{c}'$ being reflected with a new velocity vector $\mathbf{c}$, is generally used to describe a specific gas-surface interaction. Note that the molecular velocity $\mathbf{c}$ defined here is the sum of the macroscopic velocity $\mathbf{c_0}$ and the molecular thermal velocity $\mathbf{C}$, and the three components of $\mathbf{c}$ in Cartesian coordinates are denoted as u, v, and w, respectively. According to the definition of scattering kernel, there is a relationship between the reflected distribution function $f^r(\mathbf{C})$ and the incident distribution function $f^i(\mathbf{C}')$ as [49]

$$Vf^r(\mathbf{C}) = -\int_{V'<0} V' P_{\mathrm{CLL}}(\mathbf{c}' \rightarrow \mathbf{c}) f^i(\mathbf{C}') \, d\mathbf{C}', \quad (21)$$

where V and V' are the reflected and incident molecular thermal velocity in the normal direction, respectively, and $f^i(\mathbf{C}')$ is equal to $f^s(\mathbf{C}')$ according to the assumption that the distribution function is unchanged within the Knudsen layer.

For the CLL model, the tangential and normal scattering kernels can be written as

$$P_{\mathrm{CLL}}(u' \rightarrow u) = \frac{\beta}{\sqrt{\pi\alpha_t}} \exp\left[-\beta^2 \frac{\left(u - \sqrt{1-\alpha_t}u'\right)^2}{\alpha_t} \right], \quad (22)$$

$$\begin{aligned}
P_{\mathrm{CLL}}(v' \rightarrow v) &= \frac{2\beta^2 v}{\alpha_n} \mathrm{I}_0 \left(\frac{2\beta^2 \sqrt{1-\alpha_n} v' v}{\alpha_n} \right) \\
&\quad \times \exp\left[-\beta^2 \frac{v^2 + (1-\alpha_n)v'^2}{\alpha_n} \right], \quad (23)
\end{aligned}$$

where α_t and α_n are the two ACs of the tangential and normal energy, respectively, $\beta = \sqrt{\frac{m}{2kT_w}}$, and I_0 denotes the zeroth-order modified Bessel function,

$$\mathrm{I}_0(z) = \frac{1}{\pi} \int_0^\pi \exp(z\cos\theta) d\theta. \quad (24)$$

It can be seen from Eqs. (22) and (23) that the reflected tangential velocity follows a drift Maxwellian distribution with a mean velocity of $\sqrt{1-\alpha_t}$ times of the incident tangential velocity and a temperature of $\alpha_t T_w$, while the reflected normal velocity can be determined as the resultant of the two tangential velocity components. Note that the CLL model can also be formulated in terms of tangential momentum AC (σ_t), which relates to the tangential energy AC (α_t) as $\alpha_t = \sigma_t(2-\sigma_t)$. Compared to the Maxwell model, the advantage of the CLL model is that it can predict the lobular distributions of the reflected molecules, as shown in Fig. 2, and this scattering behavior agrees with experimental and molecular dynamics results.

Now we can derive the slip boundary conditions based on the CLL model. Compared to the derivations based on the Maxwell model, the only difference is determining the reflected flux due to specific scattering properties. With a determined distribution function of reflected molecules, the reflected flux yields

$$F^r = \int_{-\infty}^{\infty} \int_0^{\infty} \int_{-\infty}^{\infty} V\phi^r(\mathbf{C}) f^r(\mathbf{C}) \, d\mathbf{C}. \quad (25)$$
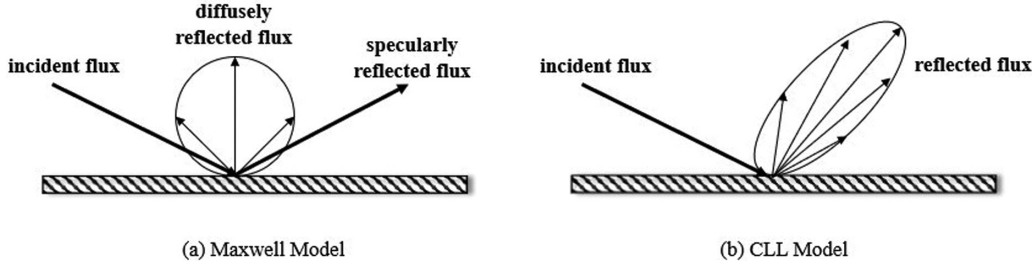
(a) Maxwell Model

(b) CLL Model

FIG. 2. Schematic of scattering properties for the Maxwell model (a) and the CLL model (b). Maxwell model is a combination of the diffusive and specular reflection, while CLL model can predict lobular distribution of the reflected molecules.

Using the relation given by Eq. (21), the reflected flux defined in Eq. (25) can be transformed to the following form:

$$F^r = \int_{-\infty}^{\infty} \int_0^{\infty} \int_{-\infty}^{\infty} V' \overline{\phi^r(\mathbf{C})} f^s(U', -V', W') \, d\mathbf{C}', \quad (26)$$

where $\overline{\phi^r(\mathbf{C})}$ is the average value of the convected quantity being reflected from the surface, that is,

$$\overline{\phi^r(\mathbf{C})} = \int_{V>0} \phi^r(\mathbf{C}) P_{\text{CLL}}(\mathbf{c}' \to \mathbf{c}) \, d\mathbf{C}. \quad (27)$$

For a gas molecule with incident tangential velocity in the x direction as $u' = (u_s + U')$, the average of reflected velocity $\overline{u}$ based on the CLL model is

$$\overline{u} = \int_{-\infty}^{\infty} u P_{\text{CLL}}(u' \to u) \, dU$$

$$= \int_{-\infty}^{\infty} u \frac{\beta}{\sqrt{\pi \alpha_t}} \exp\left[-\beta^2 \frac{(u - \sqrt{1-\alpha_t}(u_s + U'))^2}{\alpha_t}\right] du$$

$$= \sqrt{1-\alpha_t}(u_s + U'). \quad (28)$$

Consequently, the reflected momentum flux according to Eq. (26) is

$$F^r = \int_{-\infty}^{\infty} \int_0^{\infty} \int_{-\infty}^{\infty} V' m\sqrt{1-\alpha_t}(u_s + U') f^M$$

$$\times \left[1 + \frac{4\mu\beta^4}{\rho} U'V' \frac{\partial u_0}{\partial y}\right] d\mathbf{C}'$$

$$= \sqrt{1-\alpha_t} \left(\frac{n\overline{C'}}{4} m u_s + \frac{1}{2}\mu \frac{\partial u_0}{\partial y}\right). \quad (29)$$

Substituting Eqs. (9), (10), and (29) into Eq. (1), we have

$$u_s = \frac{1 + \sqrt{1-\alpha_t}}{1 - \sqrt{1-\alpha_t}} \frac{\mu \beta \sqrt{\pi}}{\rho} \frac{\partial u_0}{\partial y}. \quad (30)$$

This is the velocity slip boundary condition based on CLL model. Using the relation $\alpha_t = \sigma_t(2 - \sigma_t)$, we can transform the above equation to

$$u_s = \frac{2 - \sigma_t}{\sigma_t} \frac{\mu \beta \sqrt{\pi}}{\rho} \frac{\partial u_0}{\partial y}. \quad (31)$$

Compared to Eq. (14), it can be concluded that the CLL model predicts the same velocity slip as the Maxwell model, if the same AC is employed.

Next we derive the temperature jump condition based on the CLL model. Considering one gas molecule with incident velocity (U', V', W') without any macroscopic velocity, i.e., $\mathbf{c}' = \mathbf{C}'$, the average of the square of the reflected velocity in the x direction can be obtained as

$$\overline{u^2} = \int_{-\infty}^{\infty} u^2 P_{\text{CLL}}(u' \to u) \, du$$

$$= \int_{-\infty}^{\infty} u^2 \frac{\beta}{\sqrt{\pi \alpha_t}} \exp\left[-\beta^2 \frac{(u - \sqrt{1-\alpha_t}U')^2}{\alpha_t}\right] du$$

$$= \alpha_t \frac{kT_w}{m} + (1-\alpha_t)U'^2. \quad (32)$$

Similarly, the average of the square of the reflected velocity in the z direction is

$$\overline{w^2} = \alpha_t \frac{kT_w}{m} + (1-\alpha_t)W'^2. \quad (33)$$

And the average of the square of the reflected velocity in the normal direction is

$$\overline{v^2} = \int_0^{\infty} v^2 P_{\text{CLL}}(v' \to v) \, dv$$

$$= \int_{-0}^{\infty} v^2 \frac{2\beta^2 v}{\alpha_n} I_0\left(\frac{2\beta^2 \sqrt{1-\alpha_n}V'v}{\alpha_n}\right)$$

$$\times \exp\left[-\beta^2 \frac{v^2 + (1-\alpha_n)V'^2}{\alpha_n}\right] dv$$

$$= \alpha_n \frac{2kT_w}{m} + (1-\alpha_n)V'^2. \quad (34)$$

Consequently, the reflected energy flux according to Eq. (26) is

$$E^r = \int_{-\infty}^{\infty} \int_0^{\infty} \int_{-\infty}^{\infty} V' \frac{1}{2} m(\overline{u^2} + \overline{v^2} + \overline{w^2}) f^M$$

$$\times \left[1 + \frac{4\kappa\beta^2}{5nk}\left(\beta^2 C'^2 - \frac{5}{2}\right) V' \frac{1}{T} \frac{\partial T}{\partial y}\right] d\mathbf{C}'$$

$$= \frac{n\overline{C'}}{4}(\alpha_n + \alpha_t)kT_w + \frac{n\overline{C'}}{4}(2 - \alpha_n - \alpha_t)kT$$

$$+ \frac{5 - 3\alpha_n - 2\alpha_t}{10} \kappa \frac{\partial T}{\partial y}. \quad (35)$$

It can be seen from Eq. (35) that if $\alpha_n = \alpha_t = 0$, the predicted result automatically reduces to that predicted by Eq. (18) for the specularly reflected energy flux, while if $\alpha_n = \alpha_t = 1$, it reduces to the result predicted by Eq. (19) for the diffusively reflected energy flux.

TABLE I. Comparison of the original viscous slip coefficient C_m, the corrected viscous slip coefficient C_m^*, and the numerical results [47] for different accommodation coefficients σ_t and α_n.

σ_t	$\alpha_n = 0$			$\alpha_n = 0.5$			$\alpha_n = 1$		
	C_m	C_m^*	Ref. [47]	C_m	C_m^*	Ref. [47]	C_m	C_m^*	Ref. [47]
0.25	6.202	6.414	6.452	6.202	6.414	6.387	6.202	6.414	6.336
0.50	2.658	2.840	2.866	2.658	2.840	2.825	2.658	2.840	2.791
0.75	1.477	1.628	1.646	1.477	1.628	1.626	1.477	1.628	1.609
1	0.886	1.007	1.018	0.886	1.007	1.018	0.886	1.007	1.018

Substituting Eqs. (16), (17), and (35) into Eq. (1), we can get the temperature jump condition as follows:

$$T - T_w = \frac{2(10 - 3\alpha_n - 2\alpha_t)}{5(\alpha_n + \alpha_t)} \frac{\kappa}{kn\overline{C'}} \frac{\partial T}{\partial y}. \tag{36}$$

If $\alpha_n = \alpha_t$, then the temperature jump predicted by the above equation is consistent with the result predicted by the Maxwell model, as shown in Eq. (20). Note that it has been demonstrated by experiments and MD simulations [38,50,51], α_n and α_t are not equal in most circumstances, and their values are dependent on surface materials, surface temperature, gas temperature, gas velocity, etc. For instance, Yamamoto et al. [38] reported that the tangential and normal energy ACs are 0.52 and 0.61, respectively, for nitrogen molecules impinging on the platinum surface contaminated with xenon molecules, and thus the deviations of the temperature jump coefficients caused by the Maxwell model [Eq. (20)] and the CLL model [Eq. (36)] is about 12.7%; Spijker et al. [50] found that the tangential and normal energy ACs are 0.28 and 0.46, respectively, for argon molecules impinging on the clean platinum surface at 300 K, and thus the deviations of the temperature jump coefficients caused by these two models are up to 41.0%. It is indicated that the temperature jump boundary condition based on the CLL model is promising to give more reasonable predictions than the Maxwell model, as long as the independent values of α_n and α_t can be measured accurately.

C. Comparison of the slip coefficients

For the applications using CFD calculations, it is more convenient to express the velocity slip and temperature jump boundary conditions in general forms with slip coefficients, that is,

$$u_s = C_m \frac{\mu}{\beta p} \frac{\partial u_0}{\partial y}, \tag{37}$$

$$T - T_w = C_t \frac{\mu}{\beta p} \frac{\partial T}{\partial y}, \tag{38}$$

where p is the local pressure, and C_m and C_t are viscous slip coefficient and temperature jump coefficient, respectively. Compared the theoretical formulas derived in the present work, as shown in Eqs. (14) and (20) for the Maxwell model, to the above two equations, we can determine the theoretical slip coefficients, that is,

$$C_{m, \text{Maxwell}} = \frac{2 - \alpha}{\alpha} \frac{\sqrt{\pi}}{2}, \tag{39}$$

$$C_{t, \text{Maxwell}} = \frac{2 - \alpha}{\alpha} \frac{15\sqrt{\pi}}{16}. \tag{40}$$

Here we have used the relation between the viscosity coefficient and the thermal conductivity coefficient for monatomic gases, i.e., $\mu = \frac{4m}{15k}\kappa$, to determine the temperature jump coefficient shown in Eq. (40).

Similarly, based on the theoretical formulas derived in Eqs. (31) and (36), we can also determine the theoretical slip coefficients for the CLL model, that is,

$$C_{m, \text{CLL}} = \frac{2 - \sigma_t}{\sigma_t} \frac{\sqrt{\pi}}{2}, \tag{41}$$

$$C_{t, \text{CLL}} = \frac{2[10 - 3\alpha_n - 2\sigma_t(2 - \sigma_t)]}{5[\alpha_n + \sigma_t(2 - \sigma_t)]} \frac{15\sqrt{\pi}}{16}. \tag{42}$$

For the sake of comparison, we use the tangential momentum AC (σ_t) instead of the tangential energy AC (α_t) here.

It should be noted that the theoretical analysis performed in this work is based on the half-flux method, which assumes that within the Knudsen layer, the intermolecular collisions are negligible and the behavior of the gas is governed by the gas-surface interaction and free transport of gas molecules. It has been reported that neglecting molecular collisions within the Knudsen layer would result in the deviations of the predicted slip coefficients, and the largest deviation is about 15% [35,52]. To alleviate this deviation, Loyalka [53,54] proposed an approximate method by accounting for the variation of the distribution function within the Knudsen layer due to the effect of molecular collisions. For the Maxwell model, Loyalka determined the slip coefficients as follows [53],

$$C_{m, \text{Maxwell}}^* = \frac{2 - \alpha}{\alpha} \frac{\sqrt{\pi}}{2}(1 + 0.1366\alpha), \tag{43}$$

$$C_{t, \text{Maxwell}}^* = \frac{2 - \alpha}{\alpha} \frac{15\sqrt{\pi}}{16}(1 + 0.1621\alpha). \tag{44}$$

It can be seen that the slip coefficients determined by Loyalka are similar to the previous results for the Maxwell model, i.e., Eqs. (39) and (40), but with simple correction factors. Previous studies have demonstrated the the corrected theoretical formulas could give extremely consistent predictions with the numerical results [53].

Consider the similarity of the forms of slip coefficients for the Maxwell and CLL models derived in this work. We follow Loyalka's method and propose simple corrections to the slip coefficients for the CLL model,

$$C_{m, \text{CLL}}^* = \frac{2 - \sigma_t}{\sigma_t} \frac{\sqrt{\pi}}{2}(1 + 0.1366\sigma_t), \tag{45}$$

$$C_{t, \text{CLL}}^* = \frac{2[10 - 3\alpha_n - 2\sigma_t(2 - \sigma_t)]}{5[\alpha_n + \sigma_t(2 - \sigma_t)]} \frac{15\sqrt{\pi}}{16}(1 + 0.1621\sigma_t). \tag{46}$$
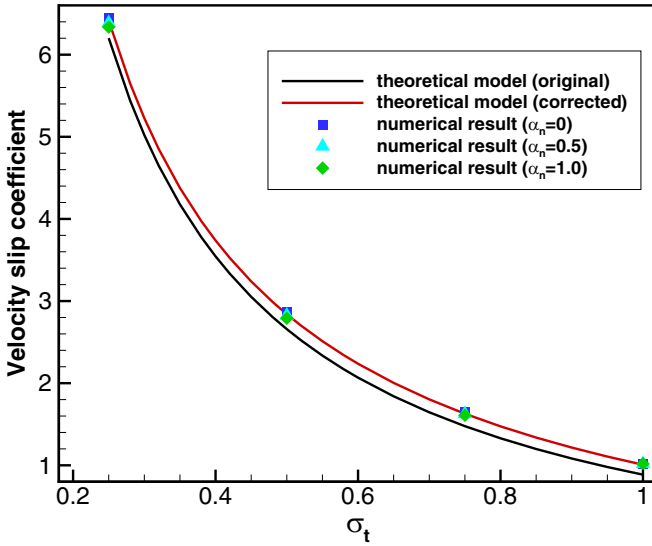
FIG. 3. Comparison of the theoretical velocity slip coefficient derived in this work and the numerical results in the literature [47]. The theoretical predictions include the original model [Eq. (41)] and the corrected model [Eq. (45)]. The abscissa is the tangential momentum accommodation coefficient.
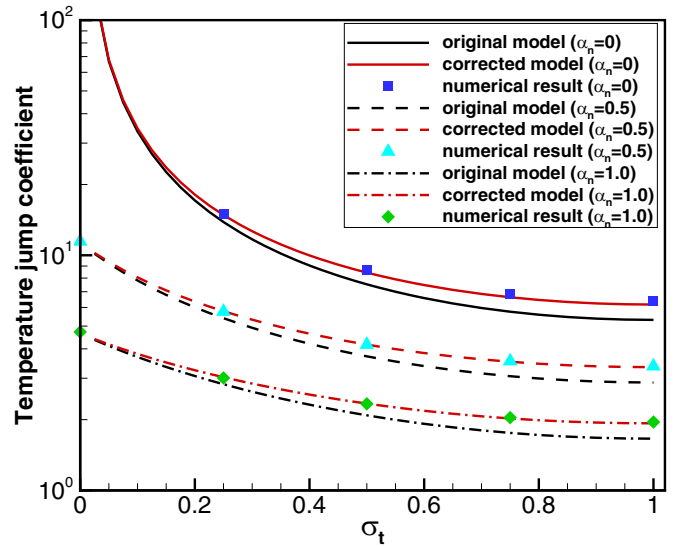

FIG. 4. Comparison of the theoretical temperature jump coefficient derived in this work and the numerical results in the literature [47]. The theoretical predictions include the original model [Eq. (42)] and the corrected model [Eq. (46)]. The abscissa is the tangential momentum accommodation coefficient.

To evaluate the accuracy of the slip coefficients determined by our theoretical models for the CLL model, we compare the original predictions given by Eqs. (41) and (42), the corrected predictions given by Eqs. (45) and (46), and the numerical results provided by Sharipov [47]. The numerical results were obtained by solving the simplified Boltzmann equation, i.e., the Shakhov model, using the discrete velocity method for the Knudsen layer.

Our theoretical models for the velocity slip, i.e., Eqs. (41) and (45), predict that the viscous slip coefficient is independent of α_n, and this behavior is confirmed by the numerical results [47], which demonstrate that the relationship between the viscous slip coefficient and α_n is very week, as shown in Fig. 3. At the same time, both our present work and the numerical results [47] predict that the viscous slip coefficient decreases as the increase of σ_t. Compared to the original theoretical model, the corrected model is more consistent with the numerical results, as shown in Fig. 3. For the sake of quantitative comparison, the data in details are presented in Table I. It can be seen that the maximum fractional error between the original viscous slip coefficient C_m and the numerical result is about 13%, while the maximum fractional error between the

corrected viscous slip coefficient C_m^* and the numerical result is less than 2%.

Figure 4 shows the comparison of the temperature jump coefficients determined by our theoretical models and numerical results for different σ_t and α_n. In contrast to the viscous slip coefficient, the temperature jump coefficient is determined by both σ_t and α_n. Basically, the theoretical models and numerical results predict that the temperature jump coefficient decreases as the increase of σ_t and α_n. Compared to the original model, the corrected model significantly improves the accuracy of prediction of the temperature jump coefficient. The data in details are presented in Table II. It can be seen that the maximum fractional error between the original temperature jump coefficient C_t and the numerical result is about 17%, while the maximum fractional error between the corrected temperature jump coefficient C_t^* and the numerical result is less than 4%.

For engineering applications, the shear stress and heat flux of the surfaces, instead of the velocity slip and temperature jump themselves, are the more important concerned quantities. Theoretically, shear stress and heat flux are proportional to the velocity gradient and the temperature

TABLE II. Comparison of the original temperature jump coefficient C_t, the corrected temperature jump coefficient C_t^*, and the numerical results [47] for different accommodation coefficients σ_t and α_n.

σ_t	$\alpha_n = 0$			$\alpha_n = 0.5$			$\alpha_n = 1$		
	C_t	C_t^*	Ref. [47]	C_t	C_t^*	Ref. [47]	C_t	C_t^*	Ref. [47]
0	—	—	—	11.29	11.29	11.45	4.648	4.648	4.722
0.25	13.85	14.83	15.03	5.400	5.784	5.763	2.829	3.030	3.009
0.50	7.525	8.440	8.653	3.718	4.170	4.170	2.087	2.340	2.335
0.75	5.755	6.629	6.855	3.060	3.525	3.549	1.756	2.023	2.040
1	5.312	6.173	6.404	2.877	3.344	3.376	1.660	1.929	1.954

gradient in the normal direction, respectively. Therefore, the relative errors of the shear stress and heat flux caused by the uncertainty of slip coefficients are generally much smaller than the values of the velocity slip and temperature jump themselves. For this reason, it can be concluded that our theoretical models with reasonable corrections could give quantitative values of the slip coefficients with an acceptable accuracy. However, solving the Boltzmann equation is computationally expensive. Moreover, for each case with specific values of σ_t and α_n, it is required for numerical method to run a separate simulation to determine the slip coefficients. Therefore, the corrected theoretical model presented in this work has big advantages in terms of computational efficiency, especially for engineering applications.

III. SLIP BOUNDARY CONDITIONS FOR BINARY MIXTURE

It is ubiquitous to encounter gas mixture flows for engineering applications, such as air flows around a hypersonic vehicle. For this reason, we further extend the above derivations to binary gas mixture. In the following, all the quantities related to a specific species are denoted with the subscript A or B. For instance, the number densities for species A and B are denoted as n_A and n_B, respectively. The viscosity and thermal conductivity coefficients for binary gas mixture are approximated as follows:

$$\mu = \frac{n_A}{n}\mu_A + \frac{n_B}{n}\mu_B, \tag{47}$$

$$\kappa = \frac{n_A}{n}\kappa_A + \frac{n_B}{n}\kappa_B. \tag{48}$$

Note that the exact formula of the transport coefficients for binary gas mixture, as summarized by Bird *et al.* [55], are more complicated than the above two equations. However, as demonstrated by Gupta *et al.* [31], these two relations are satisfied approximations for air, so they are used in this work for the sake of simplicity.

Compared to the flux balance equation [Eq. (1)] for the single species, the flux balance equation for the binary mixture is

$$F_A + F_B = F_A^i + F_B^i + F_A^r + F_B^r. \tag{49}$$

If the Maxwell model is employed for the gas-surface interaction, then the corresponding flux balance equation is

$$F_A + F_B = F_A^i + F_B^i + (1 - \alpha_A)F_A^{sp} + (1 - \alpha_B)F_B^{sp} + \alpha_A F_A^w + \alpha_B F_B^w. \tag{50}$$

In the following, we will derive the slip boundary conditions for binary gas mixture based on the Maxwell and the CLL model.

A. Slip boundary conditions for binary mixture based on the Maxwell model

Similar to the derivation of velocity slip for single-species gas, the convected property due to molecular movements is the momentum of the binary gas mixture in the x direction, $\phi = m_A(u_s + U_A') + m_B(u_s + U_B')$. We also only consider the variation of the macroscopic velocity in the y direction and neglect any temperature variation for simplicity. Consequently, the Chapman-Enskog distribution function with first-order form for species A could be written as

$$f_A^s = f_A^M\left[1 - \frac{4\mu_A\beta_A^4}{nm_A}U_A'V_A'\frac{\partial u_0}{\partial y}\right], \tag{51}$$

where n is the total number density of binary gas mixture, i.e., $n = n_A + n_B$, and $f_A^{(M)}$ is the equilibrium distribution function for species A, that is,

$$f_A^M = n_A\frac{\beta_A^3}{\pi^{3/2}}\exp\left(-\beta_A^2 C_A'^2\right). \tag{52}$$

Note that species B has the same form of distribution function as species A.

The incident momentum flux of species A is

$$\begin{aligned} F_A^i &= \int_{-\infty}^{\infty}\int_{-\infty}^{0}\int_{-\infty}^{\infty} V_A'm_A(u_s + U_A')f_A^M \\ &\quad \times\left[1 - \frac{4\mu_A\beta_A^4}{nm_A}U_A'V_A'\frac{\partial u_0}{\partial y}\right]d\mathbf{C}_A' \\ &= -\frac{n_A\overline{C_A'}}{4}m_A u_s - \frac{1}{2}\mu_A\frac{n_A}{n}\frac{\partial u_0}{\partial y}. \end{aligned} \tag{53}$$

The net flux of species A can be obtained by the integration over the whole velocity space, and the result goes to

$$F_A = -\mu_A\frac{n_A}{n}\frac{\partial u_0}{\partial y}. \tag{54}$$

For the Maxwell model, the reflected fluxes due to specular reflection and diffuse reflection for the species A can be determined easily, that is,

$$F_A^{sp} = -F_A^i, \tag{55}$$

$$F_A^w = 0. \tag{56}$$

Substituting the above four equations for the species A and the similar equations for the species B into the flux balance equation [Eq. (50)], we have

$$u_s = \frac{2[(2 - \alpha_A)\mu_A n_A + (2 - \alpha_B)\mu_B n_B]}{n(\alpha_A n_A\overline{C_A'}m_A + \alpha_B n_B\overline{C_B'}m_B)}\frac{\partial u_0}{\partial y}. \tag{57}$$

If we assume that the two species have the same ACs, that is, $\alpha_A = \alpha_B = \alpha$, then the above equation can be simplified as

$$u_s = \frac{2 - \alpha}{\alpha}\frac{2\mu}{n_A\overline{C_A'}m_A + n_B\overline{C_B'}m_B}\frac{\partial u_0}{\partial y}, \tag{58}$$

where the formula for the viscosity of binary gas mixture [Eq. (47)] has been employed. Using the relation $\overline{C_A'} = \sqrt{\frac{8kT}{\pi m_A}}$ and $\overline{C_B'} = \sqrt{\frac{8kT}{\pi m_B}}$, the above equation can also be written as

$$u_s = \frac{2 - \alpha}{\alpha}\sqrt{\frac{\pi}{2kT}}\frac{\mu}{n_A\sqrt{m_A} + n_B\sqrt{m_B}}\frac{\partial u_0}{\partial y}, \tag{59}$$

This form is consistent with that presented by Gupta *et al.* [31] for the binary gas mixture if the concerned two species have the same ACs.

Next we derive temperature jump boundary condition for binary gas mixture based on the Maxwell model. The

convected property due to molecular movements is the translational energy of molecules, i.e., $\phi = \frac{1}{2}m_A C_A'^2 + \frac{1}{2}m_B C_B'^2$. We suppose that the temperature varies only in the y direction and neglect any velocity variation, then the first-order Chapman-Enskog distribution function for species A can be written as

$$f_A^s = f_A^M\left[1 - \frac{4\kappa_A \beta_A^2}{5nk}\left(\beta_A^2 C_A'^2 - \frac{5}{2}\right)V_A' \frac{1}{T}\frac{\partial T}{\partial y}\right], \quad (60)$$

where κ_A is the thermal conductivity coefficient of species A.

The incident energy flux of species A is

$$E_A^i = \int_{-\infty}^{\infty}\int_{-\infty}^{0}\int_{-\infty}^{\infty} V_A' \frac{1}{2}m_A C_A'^2 f_A^M$$
$$\times \left[1 - \frac{4\kappa_A \beta_A^2}{5nk}\left(\beta_A^2 C_A'^2 - \frac{5}{2}\right)V_A'\frac{1}{T}\frac{\partial T}{\partial y}\right]d\mathbf{C}_A'$$
$$= -\frac{n_A\overline{C_A'}}{4}2kT - \frac{1}{2}\kappa_A \frac{n_A}{n}\frac{\partial T}{\partial y}. \quad (61)$$

Similarly, the net energy flux, the specularly reflected energy flux, and the diffusely reflected energy flux can be determined as follows:

$$E_A = -\kappa_A \frac{n_A}{n}\frac{\partial T}{\partial y}, \quad (62)$$

$$E_A^{sp} = -E_A^i, \quad (63)$$

$$E_A^w = \frac{n_A\overline{C_A'}}{4}2kT_w. \quad (64)$$

Substituting the above four equations for the species A and species B into the flux balance equation [Eq. (50)], we have

$$T - T_w = \frac{(2-\alpha_A)\kappa_A n_A + (2-\alpha_B)\kappa_B n_B}{nk(\alpha_A n_A \overline{C_A'} + \alpha_B n_B \overline{C_B'})}\frac{\partial T}{\partial y}. \quad (65)$$

Also, if we assume that these two species have the same ACs, then the above equation can be simplified as

$$T - T_w = \frac{2-\alpha}{\alpha}\frac{\kappa}{k(n_A\overline{C_A'} + n_B\overline{C_B'})}\frac{\partial T}{\partial y}. \quad (66)$$

Using the relation $\overline{C_A'} = \sqrt{\frac{8kT}{\pi m_A}}$ and $\overline{C_B'} = \sqrt{\frac{8kT}{\pi m_B}}$, the temperature jump boundary condition based on the Maxwell model can also be written as

$$T - T_w = \frac{2-\alpha}{\alpha}\sqrt{\frac{\pi}{8kT}}\frac{\kappa}{k(n_A/\sqrt{m_A} + n_B/\sqrt{m_B})}\frac{\partial T}{\partial y}. \quad (67)$$

B. Slip boundary conditions for binary mixture based on the CLL model

To derive the slip boundary conditions for binary gas mixture based on the CLL model, the crucial step is to obtain the reflected momentum flux and energy flux. For simplicity, we assume that these two species have the same ACs but each has different tangential and normal energy ACs. Following the above analyses, the reflected velocity of species A based on the CLL model can be written as

$$\overline{u_A} = \sqrt{1-\alpha_t}(u_s + U_A'). \quad (68)$$

Consequently, the reflected momentum flux of species A is

$$F_A^r = \int_{-\infty}^{\infty}\int_{0}^{\infty}\int_{-\infty}^{\infty} V_A' m_A \sqrt{1-\alpha_t}(u_s + U_A')f_A^M$$
$$\times \left[1 + \frac{4\mu_A \beta_A^4}{nm_A}U_A'V_A'\frac{\partial u_0}{\partial y}\right]d\mathbf{C}_A'$$
$$= \sqrt{1-\alpha_t}\left(\frac{n_A\overline{C_A'}}{4}m_A u_s + \frac{1}{2}\mu_A \frac{n_A}{n}\frac{\partial u_0}{\partial y}\right). \quad (69)$$

Substituting Eqs. (53), (54), and (69) into Eq. (49), we can obtain the velocity slip for binary gas mixture as

$$u_s = \frac{1 + \sqrt{1-\alpha_t}}{1 - \sqrt{1-\alpha_t}}\sqrt{\frac{\pi}{2kT}}\frac{\mu}{n_A\sqrt{m_A} + n_B\sqrt{m_B}}\frac{\partial u_0}{\partial y}. \quad (70)$$

To derive the temperature jump boundary condition, we first determine the average values of the square of the reflected velocity components for species A according to Eqs. (32)–(34), that is,

$$\overline{u_A^2} = \alpha_t \frac{kT_w}{m_A} + (1-\alpha_t)U_A'^2, \quad (71)$$

$$\overline{w_A^2} = \alpha_t \frac{kT_w}{m_A} + (1-\alpha_t)W_A'^2, \quad (72)$$

$$\overline{v_A^2} = \alpha_n \frac{2kT_w}{m_A} + (1-\alpha_n)V_A'^2. \quad (73)$$

Consequently, the reflected energy flux for species A is

$$E_A^r = \int_{-\infty}^{\infty}\int_{0}^{\infty}\int_{-\infty}^{\infty} V_A' \frac{1}{2}m_A(\overline{u_A^2} + \overline{v_A^2} + \overline{w_A^2})f_A^M$$
$$\times \left[1 + \frac{4\kappa_A \beta_A^2}{5nk}\left(\beta_A^2 c_A'^2 - \frac{5}{2}\right)v_A'\frac{1}{T}\frac{\partial T}{\partial y}\right]d\mathbf{c}_A'$$
$$= \frac{n\overline{C_A'}}{4}(\alpha_n + \alpha_t)kT_w + \frac{n\overline{C_A'}}{4}(2 - \alpha_n - \alpha_t)kT$$
$$+ \frac{5 - 3\alpha_n - 2\alpha_t}{10}\kappa_A \frac{n_A}{n}\frac{\partial T}{\partial y}. \quad (74)$$

Substituting Eqs. (61), (62), and (74) into Eq. (49) and using Eq. (48) for the thermal conductivity of binary gas mixture, we can obtain the temperature jump boundary condition based on the CLL model as

$$T - T_w = \frac{2(10 - 3\alpha_n - 2\alpha_t)}{5(\alpha_n + \alpha_t)}$$
$$\times \sqrt{\frac{\pi}{8kT}}\frac{\kappa}{k(n_A/\sqrt{m_A} + n_B/\sqrt{m_B})}\frac{\partial T}{\partial y}. \quad (75)$$

Similar to single-species gas, if the tangential and normal energy ACs are not equal, then the temperature jump coefficients based on the CLL model, as shown in Eq. (75), would be obviously different from that based on the Maxwell model. It is known that capturing the temperature jump behavior correctly at the boundary is one of the key factors to give accurate prediction of the heat flux on the surface of hypersonic vehicles. Therefore, the proposed temperature jump boundary condition based on the CLL model would be useful for the simulation of hypersonic gas flows. In addition, if the two species have different ACs, the form of the temperature jump boundary condition is more complicated than Eq. (75), but it

is can be easily derived following the above procedure. To the best of our knowledge, there are no reported slip coefficients determined by numerical results on the basis of the CLL model so far. Therefore, it is inaccessible to directly validate our results for the binary gas mixture at present, and it is expected to do in the future if massive numerical simulations based on the Boltzmann equation are performed. It is worth noting that, similar to the case of single species, we neglect molecular collisions in the analyses for binary gas mixture. Consequently, the theoretical models of the binary gas mixture also need corrections if accurate slip coefficients are required.

IV. CONCLUSIONS

We employed the half-flux method to perform theoretical analysis within the Knudsen layer, to derive the slip boundary conditions for both single-species gas and binary gas mixture based on two typical scattering kernels. If the Maxwell model is assumed for the gas-surface interaction, then the corresponding slip coefficient contains only one accommodation coefficient for both velocity slip and temperature jump. On the contrary, if the CLL model is assumed, although the derived velocity slip is the same as that predicted by the Maxwell model, then the derived temperature jump contains two accommodation coefficients in the tangential and normal directions. It has been demonstrated by experiments and molecular dynamics simulations that the tangential and normal accommodation coefficients can have obvious differences, and thus the temperature jump boundary condition derived based on the CLL model is promising to give more accurate predictions about temperature distribution and heat flux at the boundaries. To validate our theoretical models, we compared the slip coefficients predicted by our models and numerical results obtained by solving Boltzmann equation. It demonstrated that, with reasonable correction factors, the theoretical models can predict the consistent slip coefficients with the numerical results.

In this work, our analyses have only focused on single-species gas and binary gas mixture, and the extension to multicomponent mixture is straightforward. In addition, the nonequilibrium effect of internal energy during reflection from the surface and the effect of finite-rate surface catalytic recombination can also be included. Previous theoretical works [31,32] have been carried out on this subject based on the Maxwell model, and it would be meaningful, particularly for hypersonic gas flows, to extend them by taking into account the CLL scattering kernel. It should be noted that the CLL model is also not perfect at some extreme conditions, and thus it is expected to develop general slip boundary conditions based on more realistic but more complicated gas-surface interaction models [56,57].

ACKNOWLEDGMENTS

APPENDIX

1. Basic integrals for obtaining various fluxes

Here we list the the basic integrals of the distribution function needed in this work for the theoretical derivation. They are frequently used to determine the required fluxes of momentum and energy:

$$\int_0^\infty \exp\left(-\beta^2 x^2\right) dx = \frac{\sqrt{\pi}}{2\beta}, \tag{A1}$$

$$\int_0^\infty x \exp\left(-\beta^2 x^2\right) dx = \frac{1}{2\beta^2}, \tag{A2}$$

$$\int_0^\infty x^2 \exp\left(-\beta^2 x^2\right) dx = \frac{\sqrt{\pi}}{4\beta^3}, \tag{A3}$$

$$\int_0^\infty x^3 \exp\left(-\beta^2 x^2\right) dx = \frac{1}{2\beta^4}. \tag{A4}$$

2. Integrations for the incident flux

According to Eq. (9), the incident momentum flux based on the Maxwell model is

$$F^i = \int_{-\infty}^{\infty} \int_{-\infty}^{0} \int_{-\infty}^{\infty} V' m(u_s + U') n \frac{\beta^3}{\pi^{3/2}} \exp\left(-\beta^2 C'^2\right) \left[1 - \frac{4\mu\beta^4}{\rho} U'V' \frac{\partial u_0}{\partial y}\right] d\mathbf{C}'$$

$$= \int_{-\infty}^{+\infty} \int_{-\infty}^{0} \int_{-\infty}^{+\infty} nm\left(\frac{\beta^3}{\pi^{3/2}}\right) \exp\left(-\beta^2 C'^2\right) \left[u_s V' + U'V' - u_s U'V'^2 \frac{4\mu\beta^4}{\rho} \frac{\partial u_0}{\partial y} - U'^2 V'^2 \frac{4\mu\beta^4}{\rho} \frac{\partial u_0}{\partial y}\right] d\mathbf{C}'. \tag{A5}$$

Note that in the square brackets, the second and the third terms are odd functions of U' and the integration ranges are the whole velocity space, so they can be dismissed directly. The first term in the square brackets can be integrated according to Eqs. (A1) and (A2), while the fourth terms can be integrated according to Eqs. (A1) and (A3). Summing up the integration results, we have

$$F^i = -\frac{n\overline{C'}}{4} m u_s - \frac{1}{2}\mu \frac{\partial u_0}{\partial y}. \tag{A6}$$

Note that the incident energy flux based on the Maxwell model can be determined by similar procedure of integration, and it can also be obtained using software such as Wolfram Mathematica   .

[1] I. A. Leyva, Phys. Today **70**(11), 30 (2017).

[2] M. Schouler, Y. Prévereaud, and L. Mieussens, Prog. Aerosp. Sci. **118**, 100638 (2020).

[3] C. J. Greenshields and J. M. Reese, Prog. Aerosp. Sci. **52**, 80 (2012).

[4] J. J. Thalakkottor and K. Mohseni, Phys. Rev. E **94**, 023113 (2016).

[5] G. V. Candler, Annu. Rev. Fluid Mech. **51**, 379 (2019).

[6] J. Chen and H. Zhou, Acta Mech. Sin. **37**, 2 (2021).

[7] I. Nompelis, G. V. Candler, and M. S. Holden, AIAA J. **41**, 2162 (2003).

[8] H. Struchtrup, *Macroscopic Transport Equations for Rarefied Gas Flows* (Springer, Berlin, 2005).

[9] C. Shen, *Rarefied Gas Dynamics: Fundamentals, Simulations and Micro Flows* (Springer Science & Business Media, Berlin, 2006).

[10] I. D. Boyd and T. E. Schwartzentruber, *Nonequilibrium Gas Dynamics and Molecular Simulation* (Cambridge University Press, Cambridge, UK, 2017).

[11] J. Zhang, B. John, M. Pfeiffer, F. Fei, and D. Wen, Adv. Aerodyn. **1**, 12 (2019).

[12] T. Gökçen, R. W. MacCormack, and D. R. Chapman, in *AIAA Paper* (1987), p. 1115.

[13] P. M. Bhide, N. Singh, T. E. Schwartzentruber, I. Nompelis, and G. V. Candler, in *Proceedings of the 2018 AIAA Aerospace Sciences Meeting* (2018), p. 1235.

[14] J. H. Guo, G. P. Lin, J. Zhang, X. Q. Bu, and H. Li, Aerosp. Sci. Technol. **93**, 105296 (2019).

[15] J. C. Maxwell, Philos. Trans. R. Soc. London **170**, 231 (1879).

[16] T. Gökçen and R. W. MacCormack, in *AIAA Paper* (1989), p. 0461.

[17] R. G. Deissler, Int. J. Heat Mass Transfer **7**, 681 (1964).

[18] N. G. Hadjiconstantinou, Phys. Fluids **15**, 2352 (2003).

[19] D. A. Lockerby, J. M. Reese, D. R. Emerson, and R. W. Barber, Phys. Rev. E **70**, 017303 (2004).

[20] A. Beskok, Numer. Heat Transfer, Part B: Fundamentals **40**, 451 (2001).

[21] G. Karniadakis, A. Beskok, and N. Aluru, *Microflows and Nanoflows: Fundamentals and Simulation* (Springer Science & Business Media, Berlin, 2006).

[22] Z. Guo, J. Qin, and C. Zheng, Phys. Rev. E **89**, 013021 (2014).

[23] R. S. Myong, Phys. Fluids **16**, 104 (2004).

[24] N. T. P. Le, C. White, J. M. Reese, and R. S. Myong, Int. J. Heat Mass Transfer **55**, 5032 (2012).

[25] N. T. P. Le, N. H. Tran, T. N. Tran, and T. T. Tran, Proc. Inst. Mech. Eng., Part G: J. Aerosp. Eng. **234**, 840 (2020).

[26] D. A. Lockerby, J. M. Reese, and M. A. Gallis, AIAA J. **43**, 1391 (2005).

[27] C. R. Lilley and J. E. Sader, Phys. Rev. E **76**, 026315 (2007).

[28] W. Li, L. S. Luo, and J. Shen, Comput. Fluids **111**, 18 (2015).

[29] S. D. Jiang and L. S. Luo, J. Comput. Phys. **316**, 416 (2016).

[30] C. D. Scott, AIAA J. **13**, 1271 (1975).

[31] R. N. Gupta, C. D. Scott, and J. N. Moss, NASA Tech. Paper **2452** (1985).

[32] D. E. Rosner and D. H. Papadopoulos, Ind. Eng. Chem. Res. **35**, 3210 (1996).

[33] B. Xu and Y. G. Ju, Combust. Theor. Model. **10**, 961 (2006).

[34] L. Wu and H. Struchtrup, J. Fluid Mech. **823**, 511 (2017).

[35] H. Struchtrup, Phys. Fluids **25**, 112001 (2013).

[36] N. Yamanishi, Y. Matsumoto, and K. Shobatake, Phys. Fluids **11**, 3540 (1999).

[37] D. Bruno, M. Cacciatore, S. Longo, and M. Rutigliano, Chem. Phys. Lett. **320**, 245 (2000).

[38] K. Yamamoto, H. Takeuchi, and T. Hyakutake, Phys. Fluids **18**, 046103 (2006).

[39] T. F. Liang, Q. Li, and W. J. Ye, Phys. Rev. E **88**, 013009 (2013).

[40] C. Cercignani and M. Lampis, Transp. Theory Stat. Phys. **1**, 101 (1971).

[41] R. G. Lord, Phys. Fluids A **3**, 706 (1991).

[42] R. G. Lord, J. Fluid Mech. **239**, 449 (1992).

[43] N. A. Mehta and D. A. Levin, J. Thermophys. Heat Transfer **31**, 757 (2017).

[44] N. Andric, D. W. Meyer, and P. Jenny, Phys. Fluids **31**, 067109 (2019).

[45] S. K. Loyalka, Phys. Fluids A **1**, 403 (1989).

[46] S. Takata, S. Yasuda, S. Kosuge, and K. Aoki, Phys. Fluids **15**, 3745 (2003).

[47] F. Sharipov, Eur. J. Mech. B. Fluids **22**, 133 (2003).

[48] F. Sharipov, J. Phys. Chem. Ref. Data **40**, 023101 (2011).

[49] F. Sharipov, *Rarefied Gas Dynamics: Fundamentals for Research and Practice* (John Wiley & Sons, New York, NY, 2015).

[50] P. Spijker, A. J. Markvoort, S. V. Nedea, and P. A. J. Hilbers, Phys. Rev. E **81**, 011203 (2010).

[51] T. A. Sipkens and K. J. Daun, J. Phys. Chem. C **122**, 20431 (2018).

[52] R. W. Barber and D. R. Emerson, Heat Transfer Eng. **27**, 3 (2006).

[53] S. K. Loyalka, Phys. Fluids **14**, 2291 (1971).

[54] I. N. Ivchenko, S. K. Loyalka, and R. Tompson, Jr., *Analytical Methods for Problems of Molecular Transport*, Vol. 83 (Springer Science & Business Media, Berlin, 2007).

[55] R. B. Bird, E. W. Stewart, and N. E. Lightfoot, *Transport Phenomena* (John Wiley & Sons, New York, NY, 2006).

[56] T. Liang, J. Zhang, and Q. Li, Phys. Fluids **33**, 082005 (2021).

[57] S. Mohammad Nejad, E. Iype, S. Nedea, A. Frijns, and D. Smeulders, Phys. Rev. E **104**, 015309 (2021).